MRI Segmentation for brain with 3D Printing for Applications neuromechanics via base edge optimization

[1] V.Kavitha, [2] T.Rohith Raj, [3] M.Aravind, [4] Immanuel Raj, [5] B.Rahul
[1] Asst professor, [2, 3, 4, 5] UG scholars, ECE Dept, Kings Engineering college, Chennai.
[2] rohithplayz13@gmail.com

Abstract—**Recent advances in computing power and additive manufacturing (3D printing) have now made possible the efficient simulation, optimization, and replication of patient-specific procedures and prosthetics for neurosurgery applications. Two very promising applications are in finite element modeling for brain injury simulation and detection and applying additive manufacturing towards brain analogues or in vivo brain modeling. While these applications are very promising, the problem still remains of efficiently segmenting imaging data for use in finite element models or 3D printing. In this project, we put forth a novel algorithm for brain MRI image segmentation that combines statistically-based segmentation techniques with partial differential equation-based methods using neuromechanical models to provide an efficient algorithm for automated brain MRI segmentation. Findings from this project show that combining these segmentation techniques can efficiently segment brain MRI at a level of accuracy required for 3D printing applications. Specifically, we show here that combining nonlinear filtering, k-means clustering, and active contour modeling can produce robust segmentation of brain MRI images. We anticipate that these results will eventually lead to the ability to simulate brain procedures and prosthetics on a patient-specific level by using the segmented images for finite element mesh generation or additive manufacturing processes. When used in conjunction with existing simulation and optimization techniques, image segmentation technology has many far-reaching applications in neurosurgery, and the results from this project have brought some of these applications closer into reach.**

I. INTRODUCTION AND MOTIVATION

The advent of data-driven medicine and modern computing power has enabled patient-specific diagnosis and treatment based on medical imaging data. However, the primary bottleneck in this workflow remains the ability to efficiently segment medical imaging data for use in simulation, modeling, and statistical analysis. Manual image segmentation for a single CT or MRI scan is a laborious process, often requiring expensive, specialized software and many hours of work to segment a single image sequence. As an image processing problem, medical image segmentation also poses many significant challenges due to noisy data, low contrast images, and large variations between patients [1].

For applications in neurosurgery and neurology, advances in finite element modeling and additive manufacturing (3D printing) have made possible the accurate simulation and construction of patient-specific brain models and analogues [2]. However, generating finite element meshes or surface models for 3D printing requires the effective segmentation of brain MRI images. Brain MRI images are particularly difficult to segment due to the low level of contrast between the brain tissue, surrounding tissue, and cerebrospinal fluid [1]. The goal of this project is to create an image processing algorithm that can effectively segment brain MRI data. We focus on segmenting for 3D printing applications—specifically for created patient specific brain analogues—because this area remains less developed.

II. RELATED WORK

Several methods of image segmentation have been proposed, which can be roughly divided into statistical techniques and partial differential equation-based techniques. The most popular statistical technique is fuzzy c-means classification, since it can effectively segment the image into separate classes of signal [3]. Other statistical techniques are more advanced and computationally intensive, such as convolutional neural networks [5]. For partial differential equation methods, there are many models based on energy minimization and level set methods. One of the most effective partial differential equation-based techniques is active contour models, which fit a spline with minimal energy to the image contours (shown in Figure 1) [6, 7]. There are also many deterministic models of edge detection based on wavelet transform or other transform methods [8]. Wavelet-based methods work by taking the discrete wavelet transform of the image and combining these to find the edges in the image, while energy minimization methods treat the edge contour as a flexible plate and seek to minimize its energy [6, 8].

194

The algorithm presented here employs a novel method of complementing iterated active contour segmentation with nonlinear filtering and then post-processing with statistical techniques to produce an improved final segmentation result. While [7] has shown that active contours in conjunction with wavelet-based edge detection can be effective for image segmentation, little work has been done on active contours in conjunction with nonlinear filters. The algorithm is designed specifically for brain MRI segmentation, and exploits the geometric properties of the brain to improve the convergence properties.
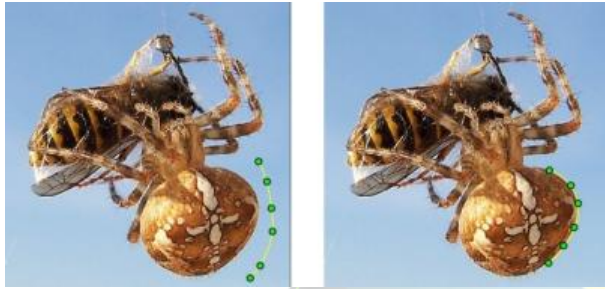

Fig. 1: Active contour models fit a spline with minimal contour energy to the image.

III. TECHNICAL APPROACH AND MATHEMATICAL FRAMEWORK

A. Active Contour Model

There currently exist two main neuromechanical models. The first is based on minimizing the distance between functionally-related neurons [9], and the other on minimizing the folding energy of cortical tissue [10]. The former hypothesis disagrees with dissection experiments, but is more in-line with the material properties of the brain. The latter model does not match material properties of the brain, but does agree well with dissection experiments. Using the latter model, from [10] we have cortical folding governed by:

$$\frac{E_c}{1-\nu_c^2}\frac{t_c^1}{12}\frac{d^1v}{ds^4} + Pt_c\frac{d^2v}{ds^2} = q$$

This differential equation gives the energy norm:

$$\alpha(s) \equiv \frac{E_c}{1-\nu_c^2}\frac{t_c^1}{12}$$

$$\beta(s) \equiv Pt_c$$

$$E = \frac{1}{2}\int_0^1\left(\alpha(s)\left(\frac{dv}{ds}\right)^2 + \beta(s)\left(\frac{d^2v}{ds^2}\right)^2\right)ds$$

Active contour models seek to minimize the energy norm of the contour [6]. Since cortical folding will naturally also seek the locally minimal energy state, there is an inherent connection between active contours and cortical folding. Because

parameterizing a contour becomes very computationally difficult due to possible topological changes in the contour as it evolves between iterations, we instead employ a level set approach from [6] and treat the contour as the zero level set of higher dimension function φ:

$$v(s) = \{(x,y)|\varphi(t=0,x,y)=0\}$$

We can then evolve φ according to the Hamilton-Jacobi equation:

$$\frac{\partial\varphi}{\partial t} = F|\nabla\varphi|$$

There are many choices for the force F. One of the simplest is:

$$\frac{\partial\varphi}{\partial t} = |\nabla\varphi|\operatorname{div}\left(\frac{\nabla\varphi}{|\nabla\varphi|}\right)$$

For this project, we used the model proposed by [11]:

$$\frac{\partial\varphi}{\partial t} = \delta_c(\varphi)\left[\mu\operatorname{div}\left(\frac{\nabla\varphi}{|\nabla\varphi|}\right) - \nu - \lambda_1(u_0-c_1)^2 + \lambda_2(u_0-c_2)^2\right] = 0$$

where c_1, c_2 are integral functions of φ, $\lambda_1 = \lambda_2 = 1$, $\nu = 0$, and μ controls the stiffness of the contour. The nonlinear PDE can be discritized and solved iteratively to converge to a local minimum (i.e. $\partial\varphi/\partial t = 0$), which will be the locally optimal active contour. This particular active contour model was chosen because it is not dependent on a large edge gradient. Due to the low contrast between gray matter and cerebrospinal fluid, the edges in brain MRI will have a low gradient, so an edge-free model is ideal for brain MRI segmentation.

B. Brain Geometry

Because the brain is a three dimensional function, we can also treat each individual slice of the brain as a level set $\Gamma(x,y)$ of a higher dimensional function $\psi(x,y,t)$. Take $\Gamma(x,y)_i = \{\psi(x,y,t)|t=h\times i\}$, $i\in Z$ and $h \equiv$ step size between brain MRI slices, and define conv(supp$\Gamma(x,y)) \equiv$ convex hull of the support of $\Gamma(x,y)$. If $\Gamma_0 \equiv$ largest MRI slice (by cross sectional area), we take $h = 1$, and there are n slices, we have:

$$\operatorname{conv}(\operatorname{supp}\Gamma_0) \subseteq \operatorname{conv}(\operatorname{supp}\Gamma_{\pm 1}) \subseteq \cdots \subseteq \operatorname{conv}(\operatorname{supp}\Gamma_{\pm n})$$

This property (approximately) holds for all brain slices, so we can exploit this property for efficiently segmenting the brain. That is, if we manually segment Γ_0, we can propagate the convex hull of each successive slice to remove unwanted features outside suppΓ_i as well as provide an accurate initial value for the active contour segmentation, which in turn accelerates the convergence.

C. *Image Segmentation Algorithm*

The proposed algorithm uses the active contour model proposed by [11]. In this algorithm, we combine gamma filtering with iterated active contour segmentation to improve the final segmentation result. Additionally, the algorithm employs statistical techniques to further remove unwanted background features and morphological post-processing to improve the 3D printing properties. The goal is to create a robust brain MRI segmentation system by combining these techniques. The algorithm is given below.

Manually segment thickest slice and initialize as Γ_0
for All slices above and below Γ_0 do

Segment S_n by $S_n^0 = S_n * \text{conv}(\text{supp}\Gamma_{n-1})$

Gamma filter: $S_n^0 = (S_n * \text{conv}(\text{supp}\Gamma_{n-1}))^{2.0}$

Initialize $\varphi_0 = \text{conv}(\text{supp}\Gamma_{n-1})$ while active contour not converged do S_n^0

  Propagate active contour on image
end while
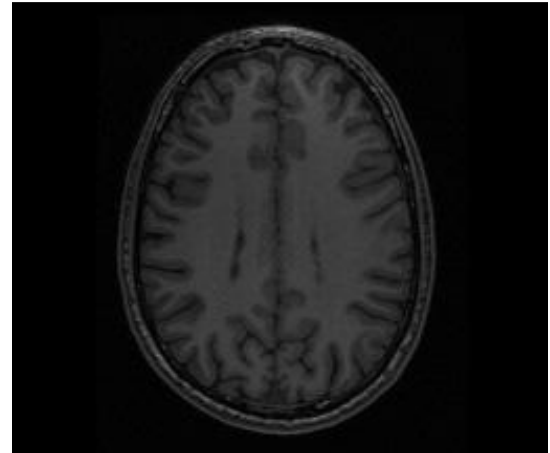
$S_n^0 = (S_n * \text{conv}(\text{supp}\Gamma_{n-1}))^{1.5}$

Initialize $\varphi_0^0 = \varphi_{converged}$

Repeat active contour iteration

Perform k-means clustering with k = 4

Record minimum centroid end for k_{avg}= average lowest centroid of k-means data Threshold each slice by k_{avg}

  Morphological post processing on segmented slices

IV. EXPERIMENTAL RESULTS

A. *Algorithm and Evaluation of System Parameters*

After manually segmenting the initial slice, first step in segmenting an intermediate slice is to load the MRI image from the image sequence. The MRI sequence contains 120 images, and the voxel size was 1mm^3.
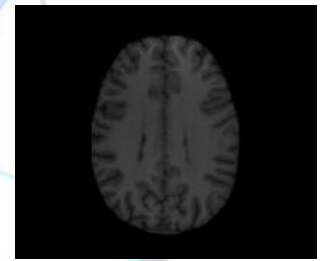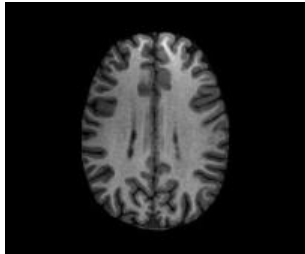

Original slice image

We can roughly segment the raw MRI image using the convex hull of the mask from the previous slice. Because the support of each successive slice is a subset of the previous slice, we can use this property to efficiently remove the skull from the image.
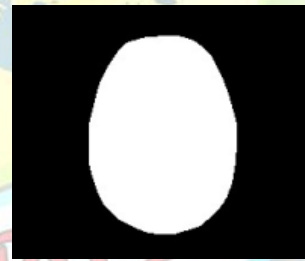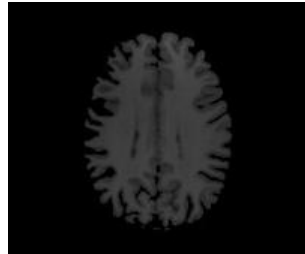

Initial Mask   Initial Segmentation

The active contour segmentation occurs in two steps. First, we apply a gamma filter with γ large to make the white matter dominant in the image. Then, we use the active contour algorithm from [11] (using the implementation in [12]) to segment the image using the gamma filter. The purpose of this step is to segment primarily the white matter, so the final contour will converge to a contour which does not contain the dura mater or other unwanted material. We found experimentally that $\gamma = 2.0$ produced good results for this step, however any γ value that sufficiently suppresses the dura mater and gray matter would be valid. Christo Ananth et al. [4] proposed a system in which an automatic anatomy segmentation method is proposed which effectively combines the Active Appearance Model, Live Wire and Graph Cut (ALG) ideas to exploit their complementary strengths. It consists of three main parts: model building, initialization, and delineation. For the initialization (recognition) part, a pseudo strategy is employed and the organs are segmented slice by slice via the OAAM (Oriented Active Appearance method). The purpose of initialization is to provide rough object localization and shape constraints for a latter GC method, which will produce refined delineation. It is better to have a fast and

robust method than a slow and more accurate technique for initialization.


Gamma Filter 1 ($\gamma = 2.0$)

Active Contour Segmentation 1

For the second active contour segmentation, we apply a gamma filter with a more moderate value ($\gamma = 1.5$ in this case), then segment with the same active contour algorithm, using the contour found in the previous step as the initial guess. The active contour converges to a locally minimal energy value, so the purpose of the first active contour segmentation is to find an initial guess for the second segmentation that will converge to the correct contour. Were we to use the convex hull of the previous slice as the initial guess, unwanted features such as the dura mater would be included in the final segmentation, and features such as separation between brain folds would be lost. For this step, we use a more flexible active contour than in the previous step i.e. do not penalize curvature as strongly in the contour optimization. From a neuromechanical standpoint, a more flexible contour when segmenting the gray matter is justified due to the lower stiffness of gray matter relative to white matter and prevalent folds in the brain structure.
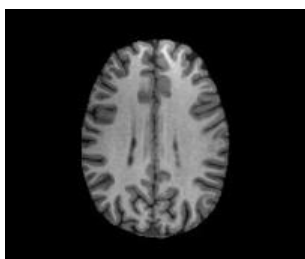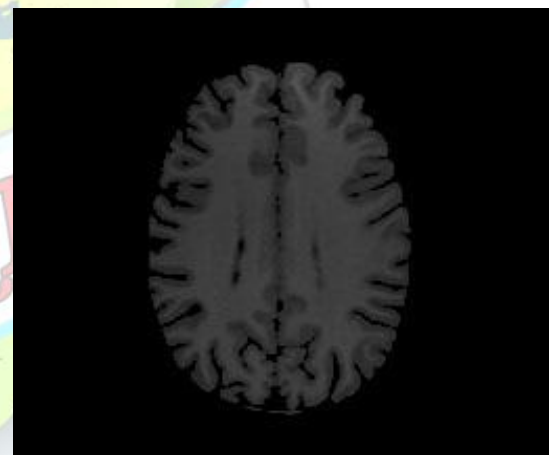

Gamma Filter 2 ($\gamma = 1.5$)
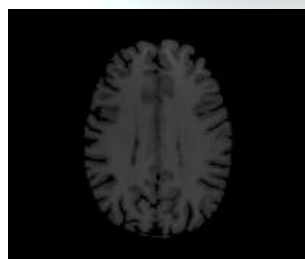
Active Contour Segmentation 2

After segmenting each slice, we perform k-means clustering on the histogram of the image using $k = 4$. For each slice, the lowest centroid was recorded. The minimum centroids were then averaged to find an average value for the background throughout the entire image sequence.

Using this average value, the segmented slices were thresholded to produce to the final binary mask.
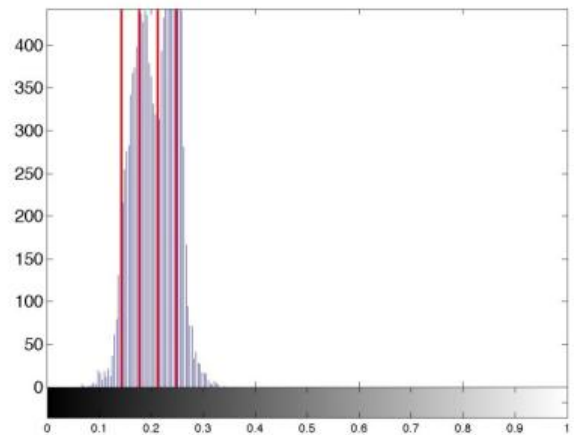

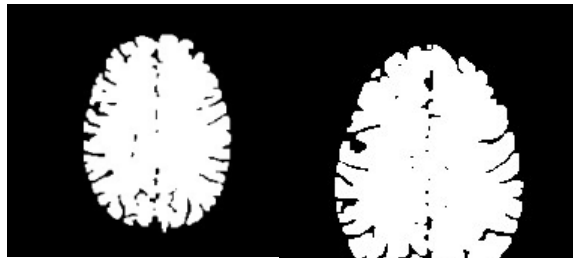Histogram after segmentation, with k-means centroids

Final segmented image

For 3D printing applications, we do post-processing on the segmented masks to remove artifacts from the thresholding. Specifically, we erode then dilate the mask. Very small or thin regions are usually artifacts and can potentially cause issues when replicating the brain sample via 3D printing since they are usually below the accuracy threshold of most commercially available printers.
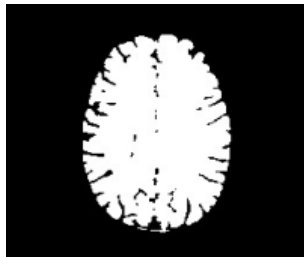
Mask before post-processing Mask after post-processing

B. Comparison to Other Approaches

Compared to manual segmentation, the given algorithm is significantly faster. Manual segmentation takes about 1-2 days of work on average, whereas this algorithm segmented the test sequence in 519 sec. (after manual segmentation of the initialization slice). The presented algorithm is very promising since its runtime is fast enough to be effective for clinical applications. The given segmentation algorithm also outperformed several existing image processing techniques. For example, figure 2 shows that the segmentation performance is worse with simple adaptive thresholding.
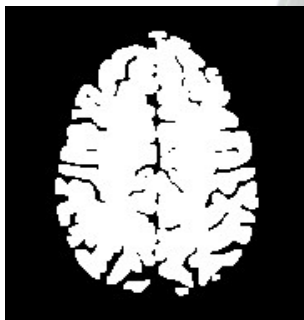

Image segmented with algorithm presented in this project. Plain adaptive thresholding via Otsu's algorithm.

Fig. 2: Comparison of presented algorithm with adaptive thresholding.

Additionally, using an edge-dependent active contour model (i.e. a model which includes a stopping function in the Hamiltonian) does not perform as well as the given algorithm. As shown by figure 3, the given algorithm is much more effective at preserving the structure of the brain slice and removing artifacts and spurious regions from thresholding. Edge-based active contour models work well where there are sharply delineated edges in an image. However, since the attenuation coefficient for cerebrospinal fluid, white matter, and gray matter are similar, there brain MRI does not have clearly delineated edges, so an edge-based active contour will perform poorly.

Image segmented with algorithm developed in this project. Image segmented with edge-dependent active contour.

Fig. 3: Comparison between presented algorithm and similar algorithm with edge-dependent active contour.
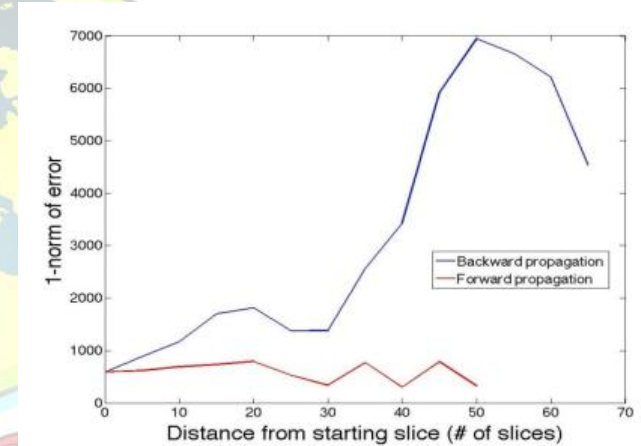

Fig. 4: Plot showing 1-norm of error with respect to distance from reference slice. Plot shows that forward propagation error grows very little, while backward propagation error grows significantly.
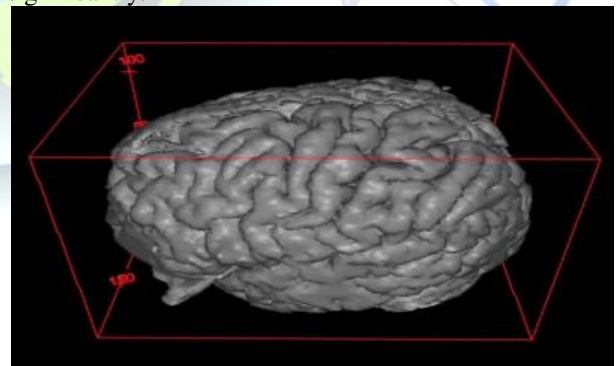

Fig. 5: Surface model generated via marching cubes method [13] using images segmented with the presented algorithm.

V. DISCUSSION

The process images show that the algorithm is able to successfully segment brain MRI images. The gamma filtering also significantly increased the performance of the active contour algorithm. This can be attributed to the nonlinearity of the gamma filter increasing the gradient of the edges, which
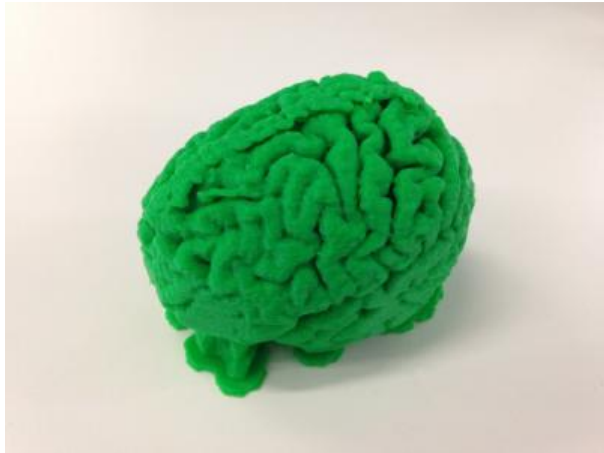

Fig. 6: Model printed via fused deposition modeling (FDM).

in turn aided the convergence of the active contour. Using kmeans clustering to find a suitable threshold for binarizing the image in the final step also yielded physically accurate results.

To quantitatively measure the error from segmentation, we first manually segmented and binarized a subset of the original brain MRI images. To evaluate the error, we used the 1-norm of the difference between the two images to measure the number of pixels that differed between the manual and automated segmentation. That is, $Error = ||I_{Manual} - I_{Automated}||_1$, where I represents the vectorized image.

Figure 4 shows the results of the error analysis. Here, we define "forward propagation" as segmenting slices that come after the reference slice in the MRI image sequence, and "backward propagation" as segmenting slices before the reference slice. The error plot shows that the errors remain relatively small for the forward propagation. This is most likely due to the well-behaved geometry of the slices segmented in the forward propagation. The error for the backwards propagation was much larger, which we attribute to two factors. First, our assumption of the brain region being compactly supported breaks down in the last slices containing the relevant brain structure e.g. in the slices containing only the temporal lobes. Secondly, in these lower slices, there are many different kinds of tissue we do not wish to segment, such as the eyes and cerebellum. These tissues were removed during the manual segmentation, but our geometric model for the brain would

not have removed these during the initial segmentation, causing significant errors in the final segmentation result.

For 3D printing applications, we were able to successfully render the segmented slices into a surface model (Figure 5) using the marching cubes method and then convert this to an STL file using [13]. The surface model was then printed using fused deposition modeling (FDM) (Figure 6). The printing results show that the morphological post-processing (edge smoothing and small region removal) improved the quality of the surface model and reduced structural errors while printing. While there are some regions of the model where details are lost, these regions are minimal and the 3D printed model is accurate enough to be used for brain analogue modeling.

VI. CONCLUSIONS AND FUTURE WORK

This project developed an algorithm that combined nonlinear filtering, active contour modeling, statistical thresholding, and morphological post-processing into a novel algorithm that can robustly segment brain MRI images. The runtime of the presented algorithm is significantly faster than manual segmentation and other existing semi-automated segmentation workflows, and the algorithm was still very effective at extracting the relevant brain tissue from the MRI images. The algorithm was less effective at removing the eyes, cerebellum, and dura mater, but these issues can be easily overcome in the future with improvements in preprocessing the image. Future work for this should focus on employing more advanced statistical techniques in the image segmentation algorithm. Two particular areas of interest are using more advanced computer vision techniques to identify and remove non-brain tissues in the lower brain slices, and use statistical learning techniques to more accurately predict the geometric evolution of the brain between slices according to the Hamilton-Jacobi equation. Overall, nonlinear filtering significantly improves the performance of active contour models in environments with weak edges, and combining statistical and morphological techniques with nonlinear filters and active contours can very efficiently segment brain MRI images at a level of accuracy suitable for neurosugery and 3D printing applications.

REFERENCES

[1] M. A. Balafar, A. R. Ramli, M. I. Saripan, and S. Mashohor, "Review of brain MRI image segmentation methods," *Artificial Intelligence Review*, vol. 33, no. 3, pp. 261–274, January 2010.

[2] M. B. Panzer, B. S. Myers, B. P. Capehart, and C. R. Bass, "Development of a finite element model for blast brain injury and the effects of CSF cavitation," *Annals of Biomedical Engineering*, vol. 40, no. 7, pp. 1530–1544, February 2012.

[3] M. Balafar, A. Ramli, M. Saripan, R. Mahmud, and S. Mashohor, "Medical image segmentation using fuzzy c-mean (fcm) and dominant grey levels of image," in *Visual Information Engineering, 2008. VIE 2008. 5th International Conference on*, July 2008, pp. 314–317.

[4] Christo Ananth, G.Gayathri, I.Uma Sankari, A.Vidhya, P.Karthiga, "Automatic Image Segmentation method based on ALG", International Journal of Innovative Research in Computer and Communication Engineering (IJIRCCE), Vol. 2, Issue 4, April 2014,pp- 3716-3721

[5] S. Khare, N. Gupta, and V. Srivastava, "Optimization technique, curve fitting and machine learning used to detect brain tumor in mri," in *Computer Communication and Systems, 2014 International Conference on*, Feb 2014, pp. 254–259.

[6] M. Kass, A. Witkin, and D. Terzopoulos, "Snakes: Active contour models," *International Journal of Computer Vision*, vol. 1, no. 4, pp. 321–331, 1988.

[7] S. W. Yoon, H. S. Shin, S. D. Min, and M. Lee, "Medical endoscopic image segmentation with multi-resolution deformation," in *2007 9th International Conference on eHealth Networking, Application and Services*. Institute of Electrical & Electronics Engineers (IEEE), June 2007.

[8] Y. Zhang, Z. Dong, L. Wu, S. Wang, and Z. Zhou,

"Feature extraction of brain MRI by stationary wavelet transform," in *2010 International Conference on Biomedical Engineering and Computer Science*. Institute of Electrical & Electronics Engineers (IEEE), April 2010.

[9] D. C. V. Essen, "A tension-based theory of morphogenesis and compact wiring in the central nervous system," *Nature*, vol. 385, no. 6614, pp. 313–318, jan 1997.

[10] S. Budday, P. Steinmann, and E. Kuhl, "The role of mechanics during brain development," *Journal of the Mechanics and Physics of Solids*, vol. 72, pp. 75–92, December 2014.

[11] T. Chan and L. Vese, "Active contours without edges," *IEEE Transactions on Image Processing*, vol. 10, no. 2, pp. 266–277, 2001.

[12] S. Lankton, "Active contour segmentation," http://www.mathworks.com/matlabcentral/fileexchange/19567acti ve-contour-segmentation, 2008–2015.

[13] W. Rasband, "Imagej," http://imagej.nih.gov/ij/, 1997– 2015.